Reconstructing contralateral fiber tracts: methodological aspects of cerebello-thalamo-cortical pathway reconstruction

Fulvia Palesi, PhD[a,b]
Jacques-Donald Tournier, PhD[c,d]
Fernando Calamante, PhD[e,f]
Nils Muhlert, PhD[g,h]
Gloria Castellazzi, PhD[b,i]
Declan Chard, MD, PhD[g,m]
Egidio D'Angelo, MD, PhD[b,l*]
Claudia Gandini Wheeler-Kingshott, PhD[g,l,n*]

[a] Department of Physics, University of Pavia, Pavia, Italy
[b] Brain Connectivity Center, C. Mondino National Neurological Institute, Pavia, Italy
[c] Department of Biomedical Engineering, Division of Imaging Sciences and Biomedical Engineering, King's College London, London, United Kingdom
[d] Centre for the Developing Brain, King's College London, London, United Kingdom
[e] The Florey Institute of Neuroscience and Mental Health, Melbourne Brain Centre, Heidelberg, Australia
[f] Department of Medicine, Austin Health and Northern Health, University of Melbourne, Heidelberg, Australia
[g] NMR Research Unit, Queen Square MS Centre, Department of Neuroinflammation, UCL Institute of Neurology, London, United Kingdom
[h] Department of Psychology, Cardiff University, Cardiff, United Kingdom
[i] Department of Industrial and Information Engineering, University of Pavia, Pavia, Italy
[l] Department of Brain and Behavioral Sciences, University of Pavia, Pavia, Italy
[m] National Institute for Health Research, University College London Hospitals Biomedical Research Centre, London, United Kingdom
[n] Brain MRI 3T Mondino Research Center, C. Mondino National Neurological Institute, Pavia, Italy

Corresponding author: Fulvia Palesi
E-mail: fulvia.palesi@unipv.it

* These two authors contributed equally to this work.

Summary

The identification of pathways connecting the cerebral cortex with subcortical structures is critical to understanding how large-scale brain networks operate. The cerebellum, for example, is known to project numerous axonal bundles to the cerebral cortex passing through the thalamus.
This paper focuses on the technical details of cerebello-thalamo-cortical pathway reconstruction using advanced diffusion MRI techniques in humans *in vivo*. Pathways reconstructed using seed/target placement on super-resolution maps, created with track density imaging (TDI), were compared with those reconstructed by defining regions of interest (ROIs) on non-diffusion weighted images (b0). We observed that the reconstruction of the pathways was more anatomically accurate when using ROIs placed on TDI rather than on b0 maps, while inter-subject variability and reproducibility were similar between the two methods. Diffusion indices along pathways showed a position-dependent specificity that will need to be taken into consideration in future clinical investigations.

KEY WORDS: cerebello-thalamo-cortical pathway, constrained spherical deconvolution, diffusion MRI, super-resolution, track-density imaging

Introduction

The role of the cerebellum in motor learning and control is well known (Evarts and Thach, 1969; Holmes, 1939), but recent research has demonstrated that it also plays a crucial role in a number of other functions, including cognition (Middleton and Strick, 1994; Schmahmann and Caplan, 2006). Understanding the connectivity between the cerebellum and cerebral regions is useful when investigating its role in these various functions. For example, studies using virus retrograde transport techniques in animals, such as mice and non-human primates, have demonstrated the presence of cerebellar connections with the prefrontal and posterior parietal cortices via the thalamus (Middleton and Strick, 2001; Ramnani, 2006; Kelly and Strick, 2003), supporting the hypothesis of a significant cerebellar role in cognition and emotion.

In vivo evidence in humans is more limited. Nevertheless, studies using advanced magnetic resonance imaging (MRI) or transcranial magnetic stimulation techniques have assessed cerebellar connectivity and plasticity through investigation of the involvement of the cerebellum in different cognitive processes (Palesi et al., 2015; Koch, 2010). In particular, the use of advanced tractography (Akhlaghi et al., 2014; Kwon et al., 2011; van Baarsen et al., 2013) has allowed the study and visualization of efferent cerebellar projections through the superior cerebellar peduncles (SCPs), the contralateral red nuclei (RN) and the thalamus to the cerebral cortex (Behrens et al., 2003; Salamon et al., 2005).

In a previous study, we combined the constrained spherical deconvolution (CSD) algorithm (Tournier et al., 2012) with probabilistic tractography as a method for reconstructing the cerebello-thalamo-cortical pathways (Palesi et al., 2015) in order to identify which cortical areas are connected with the cerebellum and quantify their specific involvement. In the present study we revisit the issue of cerebello-thalamo-cortical pathway reconstruction, describing the method in greater technical detail and illustrating how this helps us to characterize these pathways in terms of their diffusion tensor metrics. Quantification of diffusion indices along the pathways was performed with the intent of assessing whether these indices differ at different points in the pathway. This kind of information is important for comparisons in future clinical studies.

To this end, we here employed a similar approach to that used in Palesi et al. (2015) to ascertain whether: i) pathways reconstructed using seed/target placement on super-resolution images show more anatomical fidelity than those reconstructed on the basis of region placement using non-diffusion weighted images; ii) the inter-subject variability of diffusion indices along the pathway is statistically comparable between the two methods; iii) the reconstruction of the pathways is reproducible over time and between subjects. Answering these questions is a way of assessing the robustness of our cerebello-thalamo-cortical pathway reconstruction method.

Materials and methods

Subjects

The study cohort was the same as that reported in Palesi et al. (2015) and comprised subjects with no previous history of neurological symptoms: 15 right-handed healthy adults (7 males and 8 females) with a mean age of 36.1 years (range: 22–64 years). All the participants gave their written informed consent. The study protocol was approved by the local institutional research ethics board.

MRI acquisition

All data were acquired on a Philips Achieva 3T MRI scanner (Philips Healthcare, Best, Netherlands) using a 32-channel head coil as previously described by Palesi et al. (2015). The principal parameters of the high angular resolution diffusion imaging (HARDI) scan were: axial acquisition, TR ≈ 24 s (depending on the cardiac rate), TE = 68 ms, 2 mm isotropic voxel, 61 optimized non-collinear directions with a *b*-value of 1200 s/mm^2. For anatomical reference a whole brain high-resolution 3D sagittal T1-weighted (3DT1w) scan was acquired using 1 mm isotropic voxel, TR = 6.9 ms and TE = 3.1 ms.

Diffusion analysis and super-resolution map creation

HARDI data were pre-processed and aligned with the high-resolution 3DT1w images using FSL (FMRIB Software Library, http://fsl.fmrib.ox.ac.uk/fsl/fslwiki) as described in the previous work (Palesi et al., 2015). Whole brain tractography was performed using MRtrix (http://www.brain.org.au/software/mrtrix) by combining the CSD technique (Tournier et al., 2007) with probabilistic tractography and generating 2.5 million streamlines. From these streamlines a super-resolution map at 1 mm resolution was created using track-density imaging (TDI) (Calamante et al., 2010). The intensity of the TDI map was calculated as the total number of streamlines passing within each super-resolution element. TDI maps were selected due to their high spatial resolution and white matter contrast with respect to conventional diffusion tensor imaging (DTI) images.

Definition of seed and target regions of interest (ROIs)

One of the key points in cerebello-thalamo-cortical pathway reconstruction is to define appropriate seed and target ROIs in order to select pathways that are anatomically plausible. One of the possible unbiased strategies for defining seed and target ROIs is to use anatomical images, such as non-diffusion weighted (b0) or 3DT1w images. In this investigation, the use of 3DT1w images for ROI placement was not an option since no corrections were performed for EPI distortions and the area under investigation is affected by distortions, making placement unreliable. Hence, tractography results using seed and target ROIs placed on b0 were compared with those reconstructed using regions defined on super-resolution TDI maps.

The seed ROI was defined as a sphere with a 2 mm radius centered on the SCP in each cerebellar hemisphere, while a target ROI was manually drawn and placed on the contralateral RN. Seed and target ROIs were defined both on high-resolution TDI and on b0 images to identify the best image for optimal ROI placement. On the TDI map, the same method used by Palesi et al. (2015) was used: the seed ROI was identified in the coronal plane (Calamante et al., 2010), while the target ROI was identified as a very hypointense region (Calamante et al., 2013). On the

b0 image, seed location was established by visual comparison with known coordinates defined in MNI space (Anderson et al., 2011) while the target ROI was identified as a hypointense region, the hypointensity being a consequence of the region's high iron concentration (Habas and Cabanis, 2007). To assess the overlap between the target ROIs drawn on the b0 image and on the TDI map in native (subject) space the standard Dice overlap metric (Patenaude et al., 2011) was calculated.

Cerebello-thalamo-cortical tractography

For completeness, pathways were reconstructed using the ROIs defined above and standard DTI-based tractography. This was achieved by running a DTI-based deterministic tractography, selecting 3000 streamlines passing through the seed ROI (SCP). No contralateral target ROI was defined because this approach cannot resolve decussating fibers, and the streamlines produced run only ipsilaterally.
Given the limitations of DTI-based tractography in resolving crossing fibers, in this work the decussating point of the trans-hemispheric connections was resolved by combining the CSD technique with probabilistic tractography; the cerebello-thalamo-cortical pathways were reconstructed by randomly seeding streamlines throughout a seed ROI and selecting those passing through a target ROI, until 3000 streamlines had been selected. To assess the overlap between pathways reconstructed using ROIs drawn on the b0 image and on the TDI map in native (subject) space, the standard Dice overlap metric was calculated.
All subsequent analyses were run based on the CSD tractography output; therefore, from this point on, all references to reconstructed pathways are references to the outcome of this method.

Calculation of diffusion indices

Diffusion tensor components for the whole brain were calculated using MRtrix, from which fractional anisotropy (FA), mean diffusivity (MD), axial diffusivity (AD) and radial diffusivity (RD) maps were created. The mean values of all diffusion indices were calculated for each reconstructed pathway (two per subject, one for each SCP). The value of each diffusion index along each pathway for each axial slice was extracted and averaged at each slice position across subjects.

Reproducibility of ROI placement and effect on pathway reconstruction

For seven randomly chosen subjects, seed and target ROIs were redrawn by a single individual and pathways were reconstructed a second time, several months later. To test the intra-observer reproducibility of our method, the position of the ROI centers of mass was compared between the two analyses, for each placement method. On the target ROIs the standard Dice overlap metric was also calculated and compared between ROIs of the two analyses in native space, for each placement method. Furthermore, the reproducibility of the corresponding reconstructed pathways in individual subject space, from the first to the second ROI placement, was measured by thresholding the pathways, to include voxels reached at least by three streamlines and calculating the standard Dice overlap metric. An independent t-test ($p \leq 0.01$) was used to compare mean values of diffusion indices between the two pathway reconstruction trials.

Creation of mean tract maps

For all participants, 3DT1w images, previously aligned with HARDI data, were normalized to the MNI-152 template using a non-linear registration algorithm (FNIRT, FSL) (Klein et al., 2009). The same transformation was applied using nearest neighbor interpolation to seed and target ROIs and to pathways reconstructed using b0 and TDI images to assess their inter-subject overlap and consistency. The mean MNI coordinate for both seed and target ROIs was calculated for both seeding methods and for both trials in the reproducibility study. A mean image of pathways was created separately for pathways reconstructed using b0 and TDI maps starting from the binarized pathways for each subject (Ciccarelli et al., 2003a). These resulting maps were progressively thresholded to include voxels within the pathways and common to a defined percentage, i.e. 0, 20, 40, 60 and 80% of subjects.

Statistical analysis

Statistical analysis was performed using SPSS 17.0. The significance of all statistical analyses was set at $p \leq 0.01$. Individual coordinates (in mm) of the seed and target ROI centers of mass in MNI space from b0 and TDI images were compared using a paired t-test. Mean diffusion metrics of pathways reconstructed using ROIs drawn on b0 images and those of analogous tracts reconstructed using TDI maps were compared using a paired t-test. An independent t-test was used to investigate whether pathways reconstructed using ROIs drawn on b0 rather than on TDI maps showed different diffusion metrics on a slice-by-slice basis along the pathways. Another independent t-test was performed on the standard deviations of diffusion indices to test whether the inter-subject variability of diffusion indices along the pathways was statistically comparable when pathways were reconstructed using the two ROI placement methods.

Results

Figure 1 allows a qualitative comparison between seed/target ROIs (always defined on anatomical bases) on b0 images and those defined on TDI images. Figure 1b shows a schematic representation of the cerebello-thalamo-cortical pathway in order to make it easier to localize the seed/target ROIs.

Furthermore, a statistical comparison of the x, y and z coordinates (mm) of the ROI centers of mass in MNI space revealed that both seed and target ROIs placed on b0 and on TDI maps were significantly different. This difference was found for ROIs defined both during the first and the second trial. Table I reports coordinates (averaged across subjects) of seed and target ROIs and the results of the paired t-test for both trials. The location of both seed and target ROIs was significantly different ($p < 0.01$) on in-plane (i.e. x, y) but not through-plane (in feet-head direction) analysis.

Figure 2 shows a qualitative comparison between pathways reconstructed using seed/target ROIs placed on b0 and those reconstructed using seed/target ROIs placed on TDI maps. These pathways are reported at different thresholds of subjects in order to assess the influence of the threshold on spurious tracts. Figures 2a and 2b show, respectively, the mean cerebello-thalamo-cortical pathway reconstructed using ROIs placed on b0 and on TDI for both hemispheres in MNI space. Both seeding approaches resolved the decussation; however, ROIs identified on the TDI maps provided a better reconstruction capable of isolating those cerebellar pathways originating from the SCP and avoiding all other cerebellar contributors (Fig. 2c). By contrast, when using the ROIs defined on the b0 images the reconstructed pathways erroneously included cerebellar tracts running from body districts to the cerebellum and passing through the SCP (Voogd, 2008) (second to fourth image of Fig. 2d). Figure 3 shows three different axial views of the mean pathways reconstructed using TDI and b0 images, thresholded at 80% of subjects, to highlight their different extents in medial areas of the cerebellum.

Table II reports average diffusion metrics with respective standard deviations, and paired t-test results for each reconstructed pathway (from ROIs defined on the basis of b0 images or TDI maps). Mean FA and AD values were significantly increased ($p < 0.01$) for both hemispheres and for the right hemisphere, respectively, in pathways reconstructed using ROIs placed on b0 images as opposed to TDI maps. No significant differences in terms of MD and RD values were observed between pathways. For completeness, figure 4 shows boxplots relating to data reported in table II.

We performed a quantitative comparison of the pathways' average diffusion indices as a function of point along the pathway in the inferior/superior direction. Figure 1c shows that whilst FA values after the decussation are remarkably similar between the two seeding approaches, FA is increased in the slices below the decussation area in pathways generated using ROIs drawn on b0 compared with TDI. Furthermore, as shown in figure 1c, the inter-subject variability was comparable between the two methods.

Table III reports the standard Dice overlap metric calculated in the above-mentioned cases. The standard Dice overlap metric ranged from 34 to 52% when comparing target ROIs and pathways reconstructed using b0 images versus TDI maps, both for the first and the second trial. On the other hand, the Dice metric ranged from 65 to 83% in comparisons of target ROIs and pathways reconstructed during different trials of the same seeding strategy, considering ROIs placed

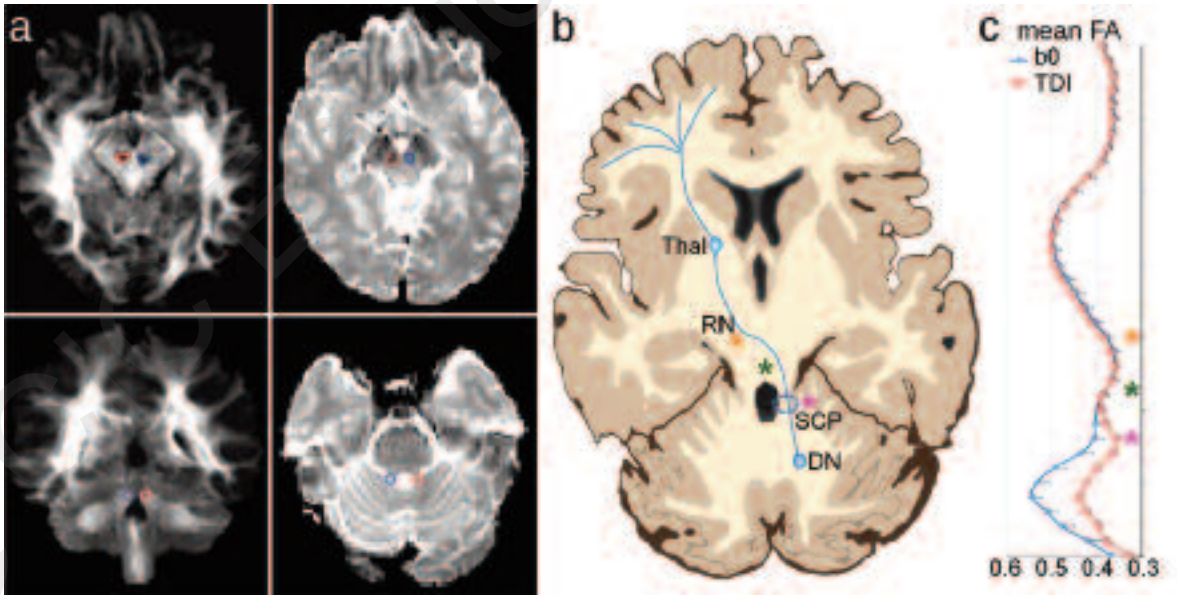

Figure 1 - Qualitative description of the cerebello-thalamo-cortical pathway reconstruction.
a) Seed/target ROI placement in a representative subject. Red indicates ROIs for left pathway while blue indicates ROIs for right pathway. From top left in a clockwise direction: contralateral target ROIs on TDI map; contralateral target ROIs on b0 image; seed ROIs on b0 image; seed ROIs on TDI map. b) Schematic representation of the cerebello-thalamo-cortical pathway. DN: dentate nucleus, SCP: superior cerebellar peduncle, RN: red nucleus, Thal: thalamus. The stars help to locate important regions on image c): the fuchsia star indicates the SCP, the green star the decussation point and the orange star the RN. c) FA profile across subjects as a function of z-position along the left pathway in MNI space. The bars represent the standard error. Red squares indicate FA values of pathways reconstructed using ROIs drawn on TDI maps. Blue diamonds indicate FA values of pathways reconstructed using ROIs drawn on b0 images.

on both b0 and TDI maps.
No significant differences were found between the seed and target ROI centers of mass of the first and the second reconstructions (Table I). Moreover, no significant differences between the diffusion metrics of the pathways reconstructed in the first and the second trial were found using an independent t-test. An example is given in figure 5, which shows the FA profile along the inferior/superior direction for pathways reconstructed in the first and the second trial.

Table I - Location of seed/target ROI centers of mass for cerebello-thalamo-cortical pathways in b0 and TDI space.

		1st experiment (15 subjects)			2nd experiment (7 subjects)		
		b0	TDI	p-value*	b0	TDI	p-value*
		Mean (SD)	Mean (SD)		Mean (SD)	Mean (SD)	
Seed ROI	Left x	–6.1 (1.1)	–4.3 (0.8)	<0.001	–6.4 (0.6)	–4.6 (1.1)	0.002
	Left y	–42.2 (1.7)	–47.6 (1.6)	<0.001	–43.3 (1.9)	–49.0 (1.3)	<0.001
	Left z	–23.4 (2.1)	–23.9 (2.0)	0.289	–24.4 (1.8)	–24.9 (2.1)	0.447
	Right x	7.4 (0.6)	5.9 (1.0)	<0.001	7.8 (0.6)	7.3 (0.7)	0.121
	Right y	–41.8 (1.4)	–47.6 (1.8)	<0.001	–43.3 (1.1)	–48.6 (1.4)	<0.001
	Right z	–22.7 (1.6)	–24.3 (2.2)	0.005	–23.7 (1.3)	–25.4 (2.2)	0.028
Target ROI	Left x	–4.2 (1.1)	–6.1 (0.8)	<0.001	–4.1 (0.5)	–6.2 (1.1)	0.002
	Left y	–20.4 (1.7)	–18.3 (1.6)	<0.001	–20.4 (1.4)	–18.1 (1.9)	0.012
	Left z	–10.1 (2.1)	–8.8 (2.0)	0.030	–10.3 (1.2)	–9.0 (1.8)	0.071
	Right x	5.5 (0.6)	4.6 (1.0)	0.008	4.3 (3.8)	4.6 (1.2)	0.835
	Right y	–20.4 (1.4)	–18.2 (1.8)	<0.001	–20.4 (0.6)	–17.7 (1.5)	0.001
	Right z	–10.1 (1.6)	–8.9 (2.2)	0.022	–10.4 (1.1)	–9.2 (1.3)	0.034

*Statistical analysis: paired t-test; $p < 0.01$ is considered significant. Values are expressed as mm coordinates in MNI-152 space.

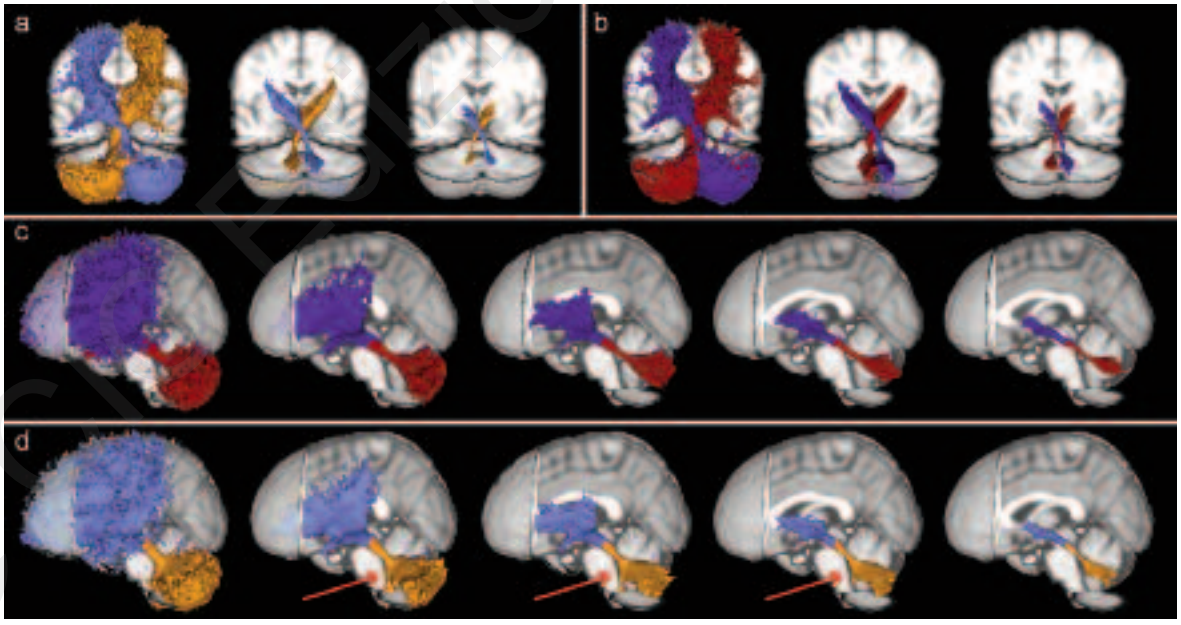

Figure 2 - Mean cerebello-thalamo-cortical pathways, across all subjects, at different thresholds of subjects.
Each tract is shown with a different color: left and right pathways are orange and light blue when b0 images were used, while they are red and blue when TDI maps were used. a) Detail of the decussation area for pathways reconstructed using ROIs on b0 images. Thresholds are (from left) equal to 0, 40 and 80% of subjects. b) Detail of the decussation area for pathways reconstructed using ROIs on TDI maps. Thresholds are (from left) equal to 0, 40 and 80% of subjects. c) Mean cerebello-thalamo-cortical pathways using ROIs on TDI maps. Thresholds are (from left) equal to 0, 20, 40, 60 and 80% of subjects. d) Mean cerebello-thalamo-cortical pathway using ROIs on b0 images. Thresholds are (from left) equal to 0, 20, 40, 60 and 80% of subjects. Red arrows indicate spino-cerebellar tracts.

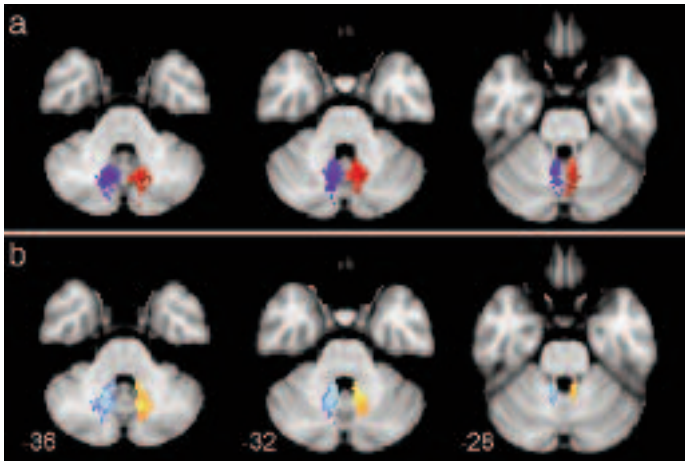

Figure 3 - Axial views of the mean cerebello-thalamo-cortical pathways, across all subjects, thresholded at 80% of subjects.
Each tract is shown with a different color: left and right pathways are orange and light blue when b0 images were used, while they are red and blue when TDI maps were used. Numbers correspond to the z coordinate (in mm) of each axial slice in MNI space.

Table II - Average diffusion index values in cerebello-thalamo-cortical pathways.

	b0	TDI	Paired t-test*
	Mean (SD)	Mean (SD)	
Left FA	0.316 (0.026)	0.303 (0.026)	**<0.001**
Right FA	0.304 (0.023)	0.295 (0.024)	**0.001**
Left MD (×10^{-3} mm^2/s)	0.821 (0.054)	0.822 (0.059)	0.781
Right MD (×10^{-3} mm^2/s)	0.829 (0.043)	0.819 (0.043)	0.058
Left AD (×10^{-3} mm^2/s)	1.090 (0.052)	1.079 (0.060)	0.155
Right AD (×10^{-3} mm^2/s)	1.095 (0.042)	1.076 (0.041)	**0.003**
Left RD (×10^{-3} mm^2/s)	0.688 (0.059)	0.696 (0.065)	0.224
Right RD (×10^{-3} mm^2/s)	0.701 (0.044)	0.696 (0.046)	0.318

Abbreviations: b0=non-diffusion weighted images; TDI=track-density imaging; SD=standard deviation; FA=fractional anisotropy; MD=mean diffusivity; AD=axial diffusivity
*Statistical analysis: $p < 0.01$ is considered significant. Significant valueV are shown in bold. Left and right refer to the seed ROI hemisphere.

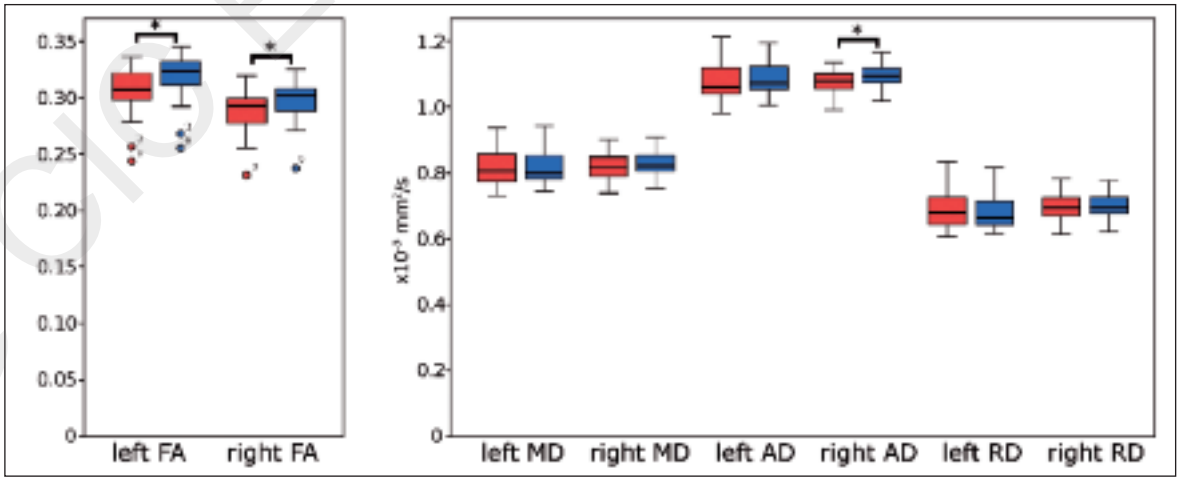

Figure 4 - Boxplots of the average diffusion metrics for left and right pathways reconstructed using ROIs placed on b0 images (blue) and on TDI maps (red).
From left: FA, MD, AD and RD values. The square brackets and stars indicate significances at $p < 0.01$.

Discussion

In this investigation, we compared an advanced method of seed/target region placement (Palesi et al., 2015), capable of precisely reconstructing the pathways connecting each cerebellar hemisphere with the contralateral cerebral cortex, with a more conventional strategy. We showed that the former leads to pathway reconstructions with higher anatomical fidelity. Our findings are in accordance with predictions based on virus transport studies in *ex vivo* animals (Voogd, 2008; Kelly and Strick, 2003) and provide one of the few *in vivo* demonstrations in humans of the crossed axonal bundles running from the cerebellar to the cerebral cortex (Kwon et al., 2011; Akhlaghi et al., 2014).
Several studies have assessed cerebellar connectivity in humans *in vivo* but few of these have used advanced diffusion techniques, e.g. diffusion spectrum imaging (Granziera et al., 2009) and CSD (Akhlaghi et al., 2014; Palesi et al., 2015), rather than the standard DTI-based reconstruction methods. As previously discussed (Palesi et al., 2015), fundamental differences between these approaches exist; in particular, unlike non-tensor model approaches, DTI-based methods fail to resolve the convergence of crossing fibers in the same area and miss all cerebellar pathways running contralaterally towards the cerebral cortex (Jissendi et al., 2008; Hyam et al., 2012) (see Fig. 3 in Palesi et al., 2015). For these reasons, we chose CSD and probabilistic tractography as our method for reconstructing the cerebello-thalamo-cortical pathways.

Table III - Standard Dice overlap metric for target ROIs and cerebello-thalamo-cortical pathways.

	Seeding comparison (TDI vs b0)		Reliability (1st vs 2nd)	
	1st test	2nd test	TDI space	b0 space
Left target ROI	34%	37%	65%	79%
Right target ROI	37%	35%	65%	83%
Left tract	51%	53%	68%	67%
Right tract	50%	52%	65%	66%

Abbreviations: ROI=region of interest; TDI=track-density imaging; b0=non-diffusion weighted images.
Values are expressed as mean percentage across subjects. Standard Dice overlap coefficients were calculated on 15 subjects for the 1st test, otherwise a sub-sample of 7 subjects was used.

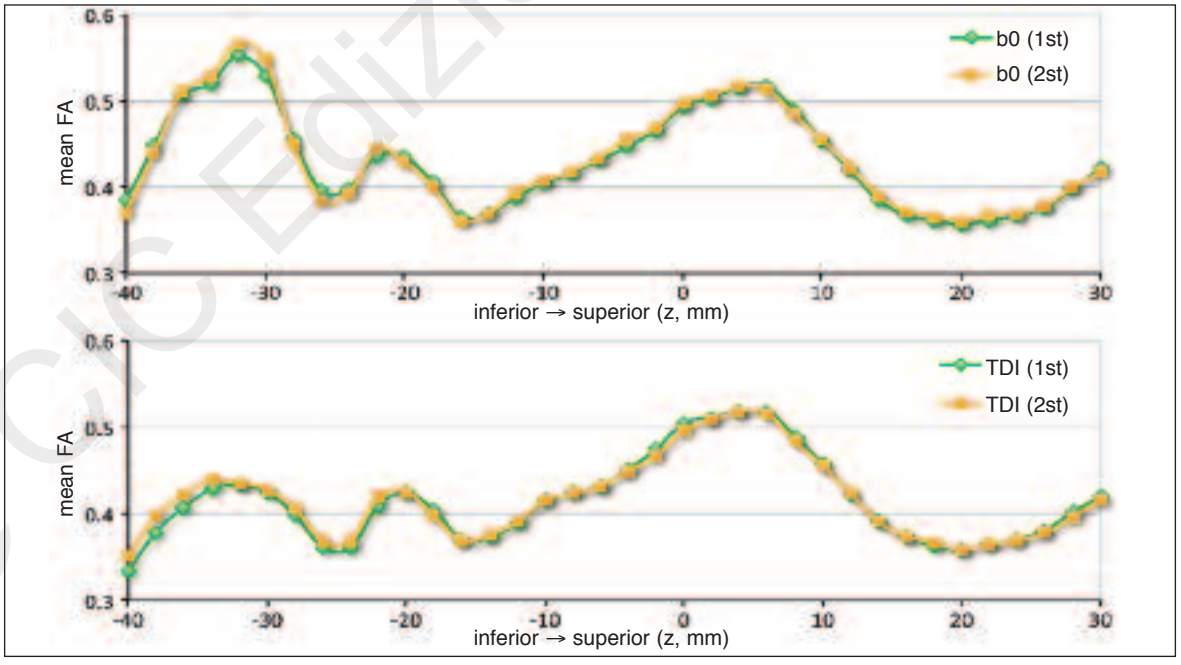

Figure 5 - FA profiles across subjects as a function of z-position along the left pathway in MNI space for the first and the second trial. Green diamonds indicate FA values of pathways reconstructed in the first trial, while orange squares indicate FA values of those reconstructed in the second trial. The top image reports FA profile for pathways reconstructed using ROIs drawn on b0 images; the bottom image reports FA profile for pathways reconstructed using ROIs drawn on TDI maps.

The placement of seed and target ROIs in native space was critical for this work. Whilst it may have been possible to define seeds using MNI coordinates, this would have introduced substantial error due to normal inter-individual variation in anatomy. Hence, the ROIs were always placed on images in native space, and predefined MNI coordinates were simply used for qualitative comparison. In particular, the method used to define ROIs was found to have a significant effect. This was noticeable in the placement of the seed and the target ROIs, based on image contrast and anatomical definition in native space. Indeed, we compared pathways reconstructed using images with different structural contrast for ROI definition, i.e. b0 images and TDI maps. Notice that FA maps were not used for selecting seed/target ROIs because despite the fact that FA is defined as a measure of diffusion anisotropy, it is not influenced solely by fine microstructure architecture. This is particularly evident in patients, in whom FA can be influenced by a number of pathological processes, e.g. the presence of lesions. Using FA maps, voxels with low anisotropy could be erroneously excluded from the seed ROI, while this is less likely when using b0 images in which the lesion can be well recognized and handled. Furthermore, it should be noted that an FA threshold (equal to 0.7) is used as a first step before performing CSD to select voxels assigned to a single-fiber mask (http://jdtournier.github.io/mrtrix-0.2/tractography/preprocess.html). Furthermore, we avoided using FA maps to draw seed/target ROIs since this is a well-recognized potential source of bias (e.g. see Ciccarelli et al., 2003b). Instead, TDI maps were chosen because they have been shown to produce rich anatomical contrast at high spatial resolution, allowing easy visualization of white matter structures (Calamante et al., 2013), and b0 images because they are anatomical images that offer an unbiased reference for diffusion EPI data. The center of mass of seed and target ROIs was found to differ between the two seeding methods. In addition, low Dice overlap metrics between target ROIs drawn on b0 images and those drawn on TDI maps further indicated the poor agreement between these approaches. This poor overlap in ROI placement also reflected differences in the reconstructed pathways. The pathways showed greater anatomical fidelity when reconstructed using seed/target ROIs drawn on TDI maps rather than b0 images; in fact some pathways not belonging to the cerebello-thalamic connections, such as the ascending ventral spino-cerebellar pathways (Fig. 2), were erroneously included in about 60% of subjects when seed/target ROIs were defined on the b0 images. Ventral spino-cerebellar pathways belong to the somatosensory system (Voogd, 2008) and are known to send proprioceptive information from body districts to the cerebellum passing through the SCP. Moreover, when seeding using TDI, tracts were found to run more medially in the cerebellum encompassing also the vermis as previously reported in studies in *ex vivo* non-human primates (Kelly and Strick, 2003). These findings suggest that the accuracy of cerebello-thalamo-cortical pathway reconstruction can be improved by using super-resolution maps, i.e. TDI maps, for defining seed ROIs. With the TDI MNI coordinates for the seed and target ROIs it may be possible, in the future, to reconstruct accurate pathways even in the absence of TDI maps. However, if MNI coordinates are used, it is imperative, always, that anatomical fidelity in native space be checked and, if necessary, adjusted for, given the small size of these ROIs and the large inter-subject variation in anatomy.

Furthermore, diffusion tensor metrics such as FA and MD were quantified along the pathways with the intent of assessing whether these indices differ at different points in the pathway. We decided to calculate these measures because this kind of information is important for comparisons in future clinical studies, performed to detect pathological changes (Anderson et al., 2011; Jeong et al., 2012; Clayden 2013). Diffusion metrics differed when reconstructing pathways using TDI maps versus b0 images. Average FA and AD values were reduced in pathways reconstructed using TDI maps. Nevertheless, when diffusion indices were expressed as a function of position along the inferior/superior direction of the pathways, they were comparable above the decussation region between pathways reconstructed using TDI and b0 images. Differences in diffusion metrics were isolated to regions below the decussation in the cerebellum where the anatomical fidelity was shown to be lower, e.g. inclusion of spino-cerebellar pathways as shown in figure 2. The influence of these tracts on FA values along cerebello-thalamo-cortical pathway was investigated by filtering them out from the pathway reconstructed using ROIs placed on b0 images. This analysis revealed that the inclusion of spino-cerebellar tracts could not explain the higher FA values along pathways reconstructed using b0 maps as seeding images. Instead, it is possible that the more medial passage of pathways seeded on TDI maps, relative to b0 images, may have resulted in a lowering of FA values (Fig.s 2a, 2b and 3).

Our results also demonstrated that no significant differences were found between pathways reconstructed from ROIs defined at different times. In particular, target placement and diffusion indices of the pathways reconstructed at different times were comparable, suggesting that our method is robust and reproducible.

Overall, despite the fact that our investigation demonstrates a robust method for reconstructing cerebello-thalamo-cortical pathways, and in general complex pathways, it suffers from well-documented shortcomings (e.g. Palesi et al., 2015). For example, MRI tractography cannot distinguish between efferent and afferent fibers, since water diffuses equally in both anterograde and retrograde directions. Furthermore, tractography cannot discriminate between direct (monosynaptic) and indirect (polysynaptic) connections between regions, because the diffusion signal is influenced by the average microstructure and not by

the presence of synapsis. Recently developed pipelines that include gray matter masks to define synaptic regions have great potential to reduce this issue in future studies (Smith et al., 2012). Another limitation when reconstructing crossing or kissing pathways is the low spatial resolution of diffusion MRI data, rarely higher than 2 mm isotropic voxels. The use of advanced approaches, e.g. combining CSD and with super-resolution TDI, can help to minimize this issue. Finally, tractography can provide only macroscopic neuroanatomical information on white matter pathways, and cannot distinguish individual axonal pathways. For this reason, reconstructed pathways cannot be claimed to be anatomically accurate on the basis of tractography alone, and results should be validated using other techniques, such as virus retrograde transport and chemical tract-tracing techniques in animals.

In conclusion, this study focuses on the technical details of cerebello-thalamo-cortical pathway reconstruction using a combination of advanced diffusion techniques. Our findings demonstrate that the use of TDI maps for seed/target ROI placement allows more anatomically accurate pathway reconstruction than does the use of a more traditional strategy, i.e. b0 images. The reproducibility of these pathways over time was good and pathway features, such as diffusion metrics and ROI locations, were comparable among subjects and were independent of when seed/target ROIs were defined.

Acknowledgments

We thank the MS Society of Great Britain and Northern Ireland, the International Spinal Research Trust, and the UCLH/UCL Comprehensive Biomedical Research Centre for funding. We also thank the C. Mondino National Neurological Institute of Pavia and University of Pavia for funding ("5 per mille, 2009" and "Ricerca Finalizzata 2008"), and the National Health and Medical Research Council (NHMRC) of Australia, the Australian Research Council (ARC) and the Victorian State Government infrastructure for their support.

References

Akhlaghi H, Yu J, Corben L, et al (2014). Cognitive deficits in Friedreich ataxia correlate with micro-structural changes in dentatorubral tract. Cerebellum 13:187-198.

Anderson VM, Wheeler-Kingshott CA, Abdel-Aziz K, et al (2011). A comprehensive assessment of cerebellar damage in multiple sclerosis using diffusion tractography and volumetric analysis. Mult Scler 17:1079-1087.

Behrens TE, Johansen-Berg H, Woolrich MW, et al (2003). Non-invasive mapping of connections between human thalamus and cortex using diffusion imaging. Nat Neurosci 6:750-757.

Calamante F, Oh SH, Tournier JD, et al (2013). Super-resolution track-density imaging of thalamic substructures: Comparison with high-resolution anatomical magnetic resonance imaging at 7.0T. Hum Brain Mapp 34:2538-2548.

Calamante F, Tournier JD, Jackson GD, et al (2010). Track-density imaging (TDI): super-resolution white matter imaging using whole-brain track-density mapping. Neuroimage 53:1233-1243.

Ciccarelli O, Toosy AT, Parker GJ, et al (2003a). Diffusion tractography based group mapping of major white-matter pathways in the human brain. Neuroimage 19:1545-1555.

Ciccarelli O, Parker GJ, Toosy AT, et al (2003b). From diffusion tractography to quantitative white matter tract measures: a reproducibility study. Neuroimage 18:348-359.

Clayden JD (2013). Imaging connectivity: MRI and the structural networks of the brain. Funct Neurol 28:197-203.

Evarts EV, Thach WT (1969). Motor mechanisms of the CNS: cerebrocerebellar interrelations. Annu Rev Physiol 31:451-498.

Granziera C, Schmahmann JD, Hadjikhani N, et al (2009). Diffusion spectrum imaging shows the structural basis of functional cerebellar circuits in the human cerebellum in vivo. PLoS One 4:e5101.

Habas C, Cabanis EA (2007). Cortical projection to the human red nucleus: complementary results with probabilistic tractography at 3 T. Neuroradiology 49:777-784.

Holmes G (1939). The cerebellum of man. Brain 62:1-30.

Hyam JA, Owen SL, Kringelbach ML, et al (2012). Contrasting connectivity of the ventralis intermedius and ventralis oralis posterior nuclei of the motor thalamus demonstrated by probabilistic tractography. Neurosurgery 70:162-169.

Jeong JW, Chugani DC, Behen ME, et al (2012). Altered white matter structure of the dentatorubrothalamic pathway in children with autistic spectrum disorders. Cerebellum 11:957-971.

Jissendi P, Baudry S, Balériaux D (2008). Diffusion tensor imaging (DTI) and tractography of the cerebellar projections to prefrontal and posterior parietal cortices: a study at 3T. J Neuroradiol 35:42-50.

Kelly RM, Strick PL (2003). Cerebellar loops with motor cortex and prefrontal cortex of a nonhuman primate. J Neurosci 23:8432-8444.

Klein A, Andersson J, Ardekani BA, et al (2009). Evaluation of 14 nonlinear deformation algorithms applied to human brain MRI registration. Neuroimage 46:786-802.

Koch G (2010). Repetitive transcranial magnetic stimulation: a tool for human cerebellar plasticity. Funct Neurol 25:159-163.

Kwon HG, Hong JH, Hong CP, et al (2011). Dentatorubrothalamic tract in human brain: diffusion tensor tractography study. Neuroradiology 53:787-791.

Middleton FA, Strick PL (2001). Cerebellar projections to the prefrontal cortex of the primate. J Neurosci 21:700-712.

Middleton FA, Strick PL (1994). Anatomical evidence for cerebellar and basal ganglia involvement in higher cognition function. Science 266:458-461.

Palesi F, Tournier JD, Calamante F, et al (2015). Contralateral cerebello-thalamo-cortical pathways with prominent involvement of associative areas in humans in vivo. Brain Struct Funct 220:3369-3384.

Patenaude B, Smith SM, Kennedy DN, et al (2011). A Bayesian model of shape and appearance for subcortical brain segmentation. Neuroimage 56:907-922.

Ramnani N (2006). The primate cortico-cerebellar system: anatomy and function. Nat Rev Neurosci 7:511-522.

Salamon N, Sicotte N, Alger J, et al (2005). Analysis of the brain-stem white-matter tracts with diffusion tensor imaging. Neuroradiology 47:895-902.

Schmahmann JD, Caplan D (2006). Cognition, emotion and the cerebellum. Brain 129:290-292.

Smith RE, Tournier J-D, Calamante F, et al. (2012). Anatomically-constrained tractography: improved diffusion MRI streamlines tractography through effective use of anatomical information. Neuroimage 62:1924-1938.

Tournier JD, Calamante F, Connelly A (2012). MRtrix: diffusion tractography in crossing fiber regions. Int J Imaging Syst Technol 22:53-66.

Tournier JD, Calamante F, Connelly A (2007). Robust determination of the fibre orientation distribution in diffusion MRI: Non-negativity constrained super-resolved spherical deconvolution. Neuroimage 35:1459-1472.

van Baarsen K, Kleinnijenhuis M, Konert T, et al (2013). Tractography demonstrates dentate-rubro-thalamic tract disruption in an adult with cerebellar mutism. Cerebellum 12:617-622.

Voogd J (2008). Cerebellum In: Standring S (Ed) Gray's Anatomy: The Anatomical Basis of Clinical Practice. London, Churchill Livingstone, pp.297-309.